

## Visual Control System for Robotic Welding

De Xu, Min Tan and Yuan Li

### 1. Introduction

In general, the teaching by showing or offline programming is used for path planning and motion programming for the manipulators. The actions preset are merely repeated in the working process. If the states of work piece varied, the manufacture quality would be influenced too intensely to satisfy the demand of production. In addition, the teaching by showing or offline programming costs much time, especially in the situations that much manufacture variety with little amount. The introduction of visual measurement in robot manufacture system could eliminate the teaching time and ensure the quality even if the state of the work piece were changed. Obviously, visual control can make the robot manufacture system have higher efficiency and better results (Bolmsjo et al., 2002; Wilson, 2002). There are many aspects concerned with the visual control for robotic welding such as vision sensor, image processing, and visual control method. As a kind of contactless seam detecting sensors, structured light vision sensor plays an important role in welding seam tracking. It has two categories. One uses structured light to form a stripe, and the other uses laser scanning. Structured light vision is regarded as one of the most promising methods because of its simplicity, higher accuracy and good performance in real-time (Wu & Chen, 2000). Many researchers pay their attention to it (Bakos et al., 1993; Zou et al., 1995; Haug & Pistrchow, 1998; Zhang & Djordjevich, 1999; Zhu & Qiang, 2000; Xu et al., 2004). For example, Bakos established a structured light measurement system, which measurement precision is 0.1mm when the distance is 500 mm. Meta Company provides many kinds of laser structured light sensors. In general, the sensor should be calibrated before putting into action. Camera calibration is an important classic topic, and a lot of literatures about it can be found (Faugeras & Toscani, 1986; Tsai, 1987; Ma, 1996; Zhang, 2000). But the procedure is complicated and tedious, especially that of the laser plane's calibration (Zhang & Djordjevich, 1999). Another problem in structured light vision is the difficulty of image processing. The structured light image of welding seam is greatly affected by strong arc light, smog and splash in the process of arc welding (Wu & Chen, 2000). Not only the image is rough, but also its background is noisy. These give rise

to difficulty, error and even failure of the processing of the welding seam image. Intelligent recognition algorithms, such as discussed in (Kim et al., 1996; Wu et al., 1996), can effectively eliminate some of the effects. However, besides intelligent recognition algorithm, it is an effective way for the improvement of recognition correctness to increase the performance of image processing.

The visual control methods fall into three categories: position-based, image-based and hybrid method (Hager et al., 1996; Corke & Good, 1996; Chaumette & Malis, 2000). As early as 1994, Yoshimi and Allen gave a system to find and locate the object with "active uncalibrated visual servoing" (Yoshimi & Allen, 1994). Experimental results by Cervera et al. demonstrated that using pixel coordinates is disadvantageous, compared with 3D coordinates estimated from the same pixel data (Cervera et al., 2002). On the other hand, although position-based visual control method such as (Corke & Good, 1993; 1996) has better stableness, it has lower accuracy than former because the errors of kinematics and camera have influence on its precision. Malis et al. proposed hybrid method that controls the translation in image space and rotation in Cartesian space. It has the advantages of two methods above (Malis et al., 1998; 1999; Chaumette & Malis, 2000).

In this chapter, a calibration method for the laser plane is presented, which is easy to be realized and provides the possibility to run hand-eye system calibration automatically. Second, the image processing methods for the laser stripe of welding seam are investigated. Third, a novel hybrid visual servoing control method is proposed for robotic arc welding with a general six degrees of freedom robot. The rest of this chapter is arranged as follows. The principle of a structured light vision sensor is introduced in Section 2. And the robot frames are also assigned in this Section. In Section 3, the laser plane equation of a structured light visual sensor is deduced from a group of rotation, in which the position of the camera's optical centre is kept unchangeable in the world frame. In Section 4, a method to extract feature points based on second order difference is proposed for type V welding seams. A main characteristic line is obtained using Hotelling transform and Hough transform. The feature points in the seam are found according to its second difference. To overcome the reflex problem, an improved method based on geometric centre is presented for multi-pass welding seams in Section 5. The profiles of welding seam grooves are obtained according to the column intensity distribution of the laser stripe image. A gravity centre detection method is provided to extract feature points on the basis of conventional corner detection method. In Section 6, a new hybrid visual control method is concerned. It consists of a position control inner loop in Cartesian space and two outer loops. One outer loop is position-based visual control in Cartesian space for moving in the direction of the welding seam, i.e. welding seam tracking; another is image-based visual control in image space for adjustment to eliminate the errors in tracking. Finally, this chapter is ended with conclusions in Section 7.

## 2. Structured light vision sensor and robot frame

### 2.1 Structured light vision sensor

The principle of visual measurement with structured light is shown in Fig. 1. A lens shaped plano-convex cylinder is employed to convert a laser beam to a plane, in order to form a stripe on the welding works. A CCD camera with a light filter is used to capture the stripe. It is a narrow band filter to allow the light in a small range with the centre of laser light wavelength to pass through. It makes the laser stripe image be very clear against the dark background. A laser emitter, a plano-convex cylinder lens, and a camera with a light filter constitute a structured light vision sensor, which is mounted on the end-effector of an arc welding robot to form a hand-eye system. The camera outputs a video signal, which is input to an image capture card installed in a computer. Then the signal is converted to image (Xu et al., 2004a).

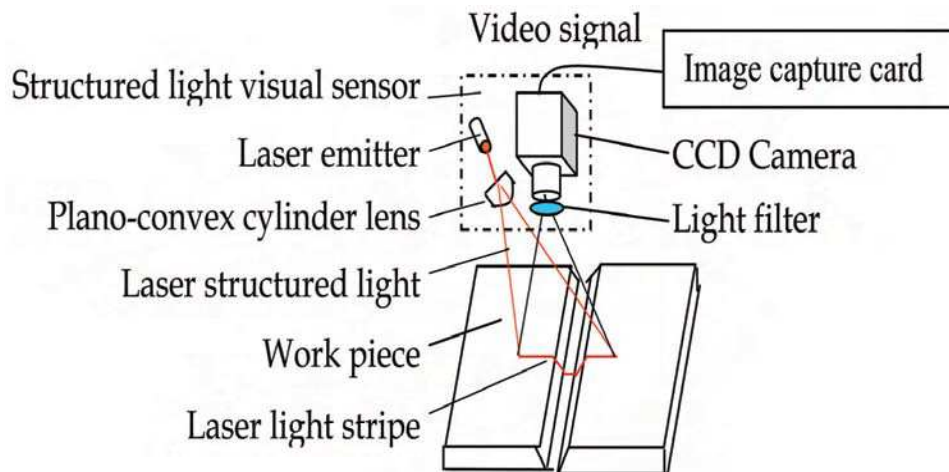


Figure 1. The principle of structured light vision sensor

### 2.2 Robot frame assignment

Coordinates frames are established as shown in Fig. 2. Frame  $W$  represents the original coordinates, i.e. the world frame. Frame  $E$  the end-effector coordinates. Frame  $R$  the working reference coordinates. Frame  $C$  the camera coordinates. The camera frame  $C$  is established as follows. Its origin is assigned at the optical centre of the camera. Its  $z$ -axis is selected to the direction of the optical axis from the camera to the scene. Its  $x$ -axis is selected as horizontal direction of its imaging plane from left to right.  ${}^wT_r$  indicates the transformation from

frame  $W$  to  $R$ , i.e. the position and orientation of frame  $R$  expressed in frame  $W$ . And  ${}^rT_c$  is from frame  $R$  to  $C$ ,  ${}^wT_e$  from frame  $W$  to  $E$ ,  ${}^eT_c$  from frame  $E$  to  $C$ .

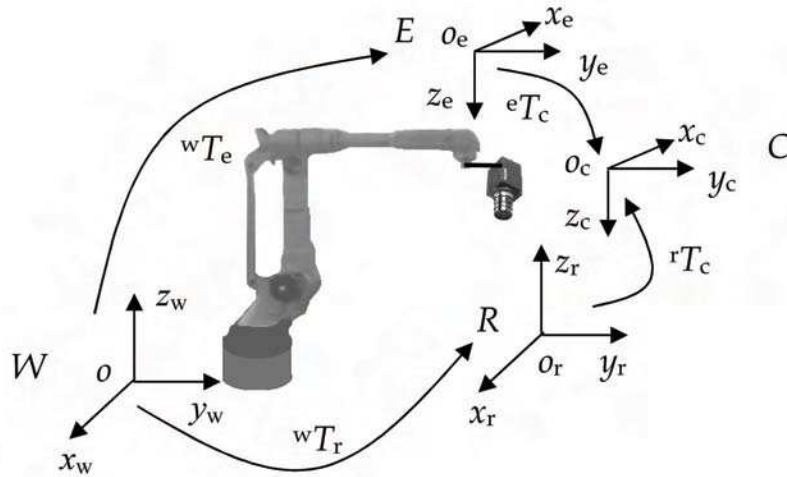


Figure 2. The sketch figure of coordinates and transformation

### 3. Laser plane calibration

#### 3.1 Calibration method based on rotation

Generally, the camera is with small view angle, and its intrinsic parameters can be described with pinhole model, as given in (1). Its extrinsic parameters can be given in (2).

$$\begin{bmatrix} u \\ v \\ 1 \end{bmatrix} = \begin{bmatrix} k_x & 0 & u_0 \\ 0 & k_y & v_0 \\ 0 & 0 & 1 \end{bmatrix} \begin{bmatrix} x_c / z_c \\ y_c / z_c \\ 1 \end{bmatrix} = M_{in} \begin{bmatrix} x_c / z_c \\ y_c / z_c \\ 1 \end{bmatrix} \quad (1)$$

where  $[u, v]$  are the coordinates of a point in an image,  $[u_0, v_0]$  denote the image coordinates of the camera's principal point,  $[x_c, y_c, z_c]$  are the coordinates of a point in the camera frame,  $M_{in}$  is the intrinsic parameters matrix, and  $[k_x, k_y]$  are the magnification coefficients from the imaging plane coordinates to the image coordinates. In fact,  $[k_x, k_y]$  are formed with the focal length and the magnification factor from the image size in mm to the imaging coordinates in pixels.

$$\begin{bmatrix} x_c \\ y_c \\ z_c \end{bmatrix} = \begin{bmatrix} n_x & o_x & a_x & p_x \\ n_y & o_y & a_y & p_y \\ n_z & o_z & a_z & p_z \end{bmatrix} \begin{bmatrix} x_w \\ y_w \\ z_w \\ 1 \end{bmatrix} = {}^cM_w \begin{bmatrix} x_w \\ y_w \\ z_w \\ 1 \end{bmatrix} \quad (2)$$

where  $[x_w, y_w, z_w]$  are the coordinates of a point in the object frame, and  ${}^cM_w$  is the extrinsic parameter matrix of the camera, i.e. the transformation from the camera frame  $C$  to the world frame  $W$ . In  ${}^cM_w$ ,  $\bar{n} = [n_x \ n_y \ n_z]^T$  is the direction vector of the  $x$ -axis,  $\bar{o} = [o_x \ o_y \ o_z]^T$  is that of the  $y$ -axis,  $\bar{a} = [a_x \ a_y \ a_z]^T$  is that of the  $z$ -axis for the frame  $W$  expressed in the frame  $C$ , and  $\bar{p} = [p_x \ p_y \ p_z]^T$  is the position vector.

Camera calibration is not a big problem today. But laser plane calibration is still difficult. Therefore, the calibration of structured light vision sensor is focused on laser plane except camera. In the following discussion (Xu & Tan, 2004), the parameters of a camera are supposed to be well calibrated in advance.

Assume the equation of the laser light plane in frame  $C$  is as follows

$$ax + by + cz + 1 = 0 \quad (3)$$

where  $a, b, c$  are the parameters of the laser light plane.

An arbitrary point  $P$  in laser stripe must be in the line formed by the lens centre and the imaging point  $[x_{c1}, y_{c1}, 1]$ . Formula (4) shows the equation of the line in frame  $C$ .

$$\begin{bmatrix} x \\ y \\ z \end{bmatrix}^T = \begin{bmatrix} x_{c1} \\ y_{c1} \\ 1 \end{bmatrix}^T t \quad (4)$$

where  $x_{c1} = x_c/z_c$ ,  $y_{c1} = y_c/z_c$ ,  $t$  is an intermediate variable.

On the other hand, the imaging point  $[x_{c1}, y_{c1}, 1]^T$  can be calculated from (1) as follows.

$$\begin{bmatrix} x_{c1} \\ y_{c1} \\ 1 \end{bmatrix}^T = M_{in}^{-1} \begin{bmatrix} u \\ v \\ 1 \end{bmatrix}^T \quad (5)$$

From (3) and (4), the coordinates of point  $P$  in frame  $C$  can be expressed as the functions of parameter  $a, b$ , and  $c$ , given in (6). Further more, its coordinates  $[x_w, y_w, z_w]$  in frame  $W$  can be had as given in (7).

$$\begin{cases} x = -x_{c1} / (ax_{c1} + by_{c1} + c) \\ y = -y_{c1} / (ax_{c1} + by_{c1} + c) \\ z = -1 / (ax_{c1} + by_{c1} + c) \end{cases} \quad (6)$$

$$[x_w \ y_w \ z_w \ 1]^T = {}^wT_e \ {}^eT_c [x \ y \ z \ 1]^T \quad (7)$$

Let

$${}^wT_e \ {}^eT_c = \begin{bmatrix} n_x & o_x & a_x & p_x \\ n_y & o_y & a_y & p_y \\ n_z & o_z & a_z & p_z \\ 0 & 0 & 0 & 1 \end{bmatrix} = \begin{bmatrix} \bar{n} & \bar{o} & \bar{a} & \bar{p} \\ 0 & 0 & 0 & 1 \end{bmatrix} \quad (8)$$

then (9) is deduced from (7) and (8).

$$\begin{cases} x_w = n_x x + o_x y + a_x z + p_x \\ y_w = n_y x + o_y y + a_y z + p_y \\ z_w = n_z x + o_z y + a_z z + p_z \end{cases} \quad (9)$$

If the surface of work piece is a plane, the points in the laser stripe will satisfy its plane equation (10).

$$Ax_w + By_w + Cz_w + 1 = 0 \quad (10)$$

in which  $A$ ,  $B$  and  $C$  are the parameters of the work piece plane in frame  $W$ . Submitting (9) to (10), then

$$\begin{aligned} & A(n_x x + o_x y + a_x z) + B(n_y x + o_y y + a_y z) + \\ & C(n_z x + o_z y + a_z z) + Ap_x + Bp_y + Cp_z + 1 = 0 \end{aligned} \quad (11)$$

Let  $D = Ap_x + Bp_y + Cp_z + 1$ . It is sure that the lens centre of the camera,  $[p_x, p_y, p_z]$ , is not on the plane of work piece. Therefore the condition  $D \neq 0$  is satisfied. Equation (11) is rewritten as (12) via divided by  $D$  and applying (6) to it (Xu & Tan, 2004).

$$\begin{aligned} & A_1(n_x x_{c1} + o_x y_{c1} + a_x) + B_1(n_y x_{c1} + o_y y_{c1} + a_y) \\ & + C_1(n_z x_{c1} + o_z y_{c1} + a_z) - ax_{c1} - by_{c1} - c = 0 \end{aligned} \quad (12)$$

here  $A_1 = A/D$ ,  $B_1 = B/D$ ,  $C_1 = C/D$ .

If the optical axis of the camera is not parallel to the plane of the laser light, then  $c \neq 0$  is satisfied. In fact, the camera must be fixed in some direction except that parallel to the plane of the laser light in order to capture the laser stripe. Dividing (12) by  $c$ , then

$$A_2(n_x x_{cl} + o_x y_{cl} + a_x) + B_2(n_y x_{cl} + o_y y_{cl} + a_y) + C_2(n_z x_{cl} + o_z y_{cl} + a_z) - a_1 x_{cl} - b_1 y_{cl} = 1 \quad (13)$$

where  $A_2 = A_1/c$ ,  $B_2 = B_1/c$ ,  $C_2 = C_1/c$ ,  $a_1 = a/c$ ,  $b_1 = b/c$ .

In the condition that the point of the lens centre  $[p_x, p_y, p_z]$  is kept unchangeable in frame  $O$ , a series of laser stripes in different directions are formed with the pose change of the vision sensor. Any point in each laser stripe on the same plane of a work piece satisfies (13). Notice the linear correlation, only two points can be selected from each stripe to submit to formula (13). They would form a group of linear equations, whose number is as two times as that of stripes. If the number of equations is greater than 5, they can be solved with least mean square method to get parameters such as  $A_2, B_2, C_2, a_1, b_1$ .

Now the task of laser calibration is to find the parameter  $c$ . The procedure is very simple. It is well known that the distance between two points  $P_i$  and  $P_j$  on the stripe is as follows

$$d = \sqrt{(x_{wi} - x_{wj})^2 + (y_{wi} - y_{wj})^2 + (z_{wi} - z_{wj})^2} = \sqrt{d_x^2 + d_y^2 + d_z^2} \quad (14)$$

in which,  $[x_{wi}, y_{wi}, z_{wi}]$  and  $[x_{wj}, y_{wj}, z_{wj}]$  are the coordinates of point  $P_i$  and  $P_j$  in the world frame;  $d_x, d_y, d_z$  are coordinates decomposition values of distance  $d$ . Submitting (6) and (9) to (14), then

$$\begin{aligned} d_x = & \frac{1}{c} \left[ n_x \left( \frac{x_{clj}}{a_1 x_{clj} + b_1 y_{clj} + 1} - \frac{x_{cli}}{a_1 x_{cli} + b_1 y_{cli} + 1} \right) \right. \\ & + o_x \left( \frac{y_{clj}}{a_1 x_{clj} + b_1 y_{clj} + 1} - \frac{y_{cli}}{a_1 x_{cli} + b_1 y_{cli} + 1} \right) \\ & \left. + a_x \left( \frac{1}{a_1 x_{clj} + b_1 y_{clj} + 1} - \frac{1}{a_1 x_{cli} + b_1 y_{cli} + 1} \right) \right] = \frac{1}{c} d_{x1} \end{aligned} \quad (15)$$

In the same way,  $d_y$  and  $d_z$  are deduced. Then

$$d = \pm \frac{1}{c} \sqrt{d_{x1}^2 + d_{y1}^2 + d_{z1}^2} = \pm \frac{1}{c} d_1 \Rightarrow c = \pm \frac{d_1}{d} \quad (16)$$

where  $d_1$  is the calculated distance between two points on the stripe with parameters  $a_1$  and  $b_1$ , and  $d$  is the measured distance with ruler.

Then parameters  $a$  and  $b$  can be directly calculated from  $c$  as formula (17). Applying  $a$ ,  $b$ , and  $c$  to (6), the sign of parameter  $c$  could be determined with the constraint  $z > 0$ .

$$\begin{cases} a = a_1 c \\ b = b_1 c \end{cases} \quad (17)$$

### 3.2 Experiment and results

The camera in the vision sensor was well calibrated in advance. Its intrinsic parameters  $M_{in}$  and extrinsic ones  ${}^eT_c$  were given as follows.

$$M_{in} = \begin{bmatrix} 2620.5 & 0 & 408.4 \\ 0 & 2619.1 & 312.2 \\ 0 & 0 & 1 \end{bmatrix}, \quad {}^eT_c = \begin{bmatrix} -0.0867 & -0.6620 & -0.7444 & 51.9160 \\ -0.0702 & 0.7495 & -0.6583 & -89.9243 \\ 0.9938 & -0.0048 & -0.1115 & 35.3765 \\ 0 & 0 & 0 & 1 \end{bmatrix}.$$

in which the image size is 768×576 pixels.

#### 3.2.1 Laser Plane Calibration

A structured light vision sensor was mounted on the end-effector of an arc welding robot to form a hand-eye system. The laser stripe was projected to a plane approximately parallel to the  $XOY$  plane in frame  $W$ . The poses of the vision sensor were changed through the end-effector of the robot for seven times. And the lens centre point  $[p_x, p_y, p_z]$  was kept unchangeable in frame  $W$  in this procedure. So there were seven stripes in different directions. Any two points were selected from each stripe to submit to (13). Fourteen linear equations were formed. Then the parameters such as  $A_2, B_2, C_2, a_1, b_1$  could be obtained from them. It was easy to calculate the length  $d_1$  of one stripe with  $a_1$  and  $b_1$ , and to measure its actual length  $d$  with a ruler. In fact, any two points on a laser stripe satisfy (14)-(16) whether the laser stripe is on a plane or not. To improve the precision of manual measure, a block with known height was employed to form a laser stripe with apparent break points, as seen in Fig. 3. The length  $d_1$  was computed from the two break points. Then parameters of the laser plane equation were directly calculated with (13)-(17). The results are as follows.



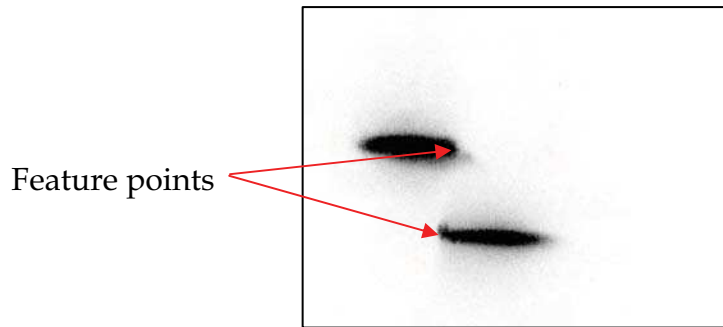


Figure 3. A laser stripe formed with a block

$$d=23\text{mm}, d_1=0.1725, a=-9.2901 \times 10^{-4}, b=2.4430 \times 10^{-2}, c=-7.5021 \times 10^{-3}.$$

So the laser plane equation in frame *C* is:  
 $-9.2901 \times 10^{-4}x + 2.4430 \times 10^{-2}y - 7.5021 \times 10^{-3}z + 1 = 0.$

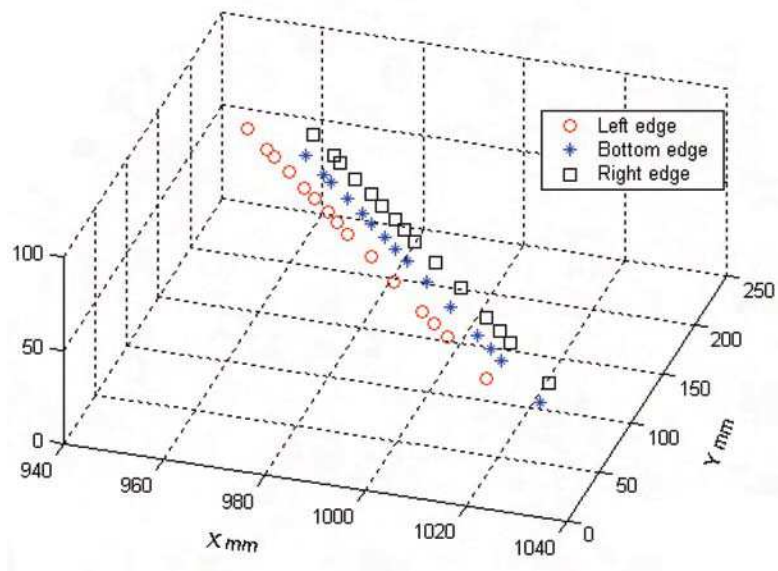
**3.2.2 The verification of the hand-eye system**

A welding seam of type V was measured by use of the structured light vision sensor to verify the hand-eye system. The measurements were conducted 15 times along the seam. Three points were selected from the laser stripe for each time, which were two edge points and a bottom one. Their coordinates in frame *W* were computed via the method proposed above. The results were shown in Table 1.

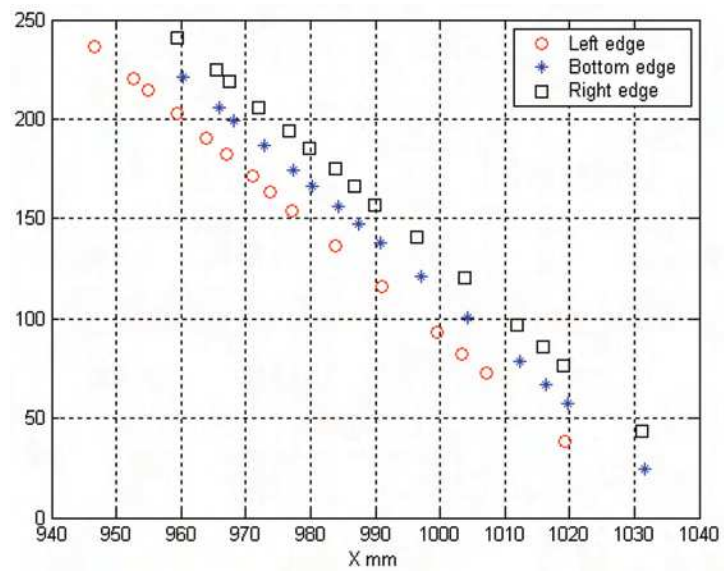
No.	1	2	3	4	5	6	7	8	9	10	11	12	13	14	15
$x_{w1}$	1019.16	1007.22	1003.34	999.55	991.11	983.95	977.16	973.85	971.13	967.05	963.89	959.34	954.90	952.73	946.64
$y_{w1}$	38.68	72.51	82.53	93.17	116.12	136.33	153.67	163.10	171.24	182.04	190.31	202.58	214.91	220.74	236.73
$z_{w1}$	47.09	46.70	46.85	46.66	46.74	46.50	46.74	46.93	46.74	46.68	46.73	46.85	46.73	46.57	46.74
$x_{w2}$	1031.54	1019.68	1016.36	1012.30	1004.21	996.99	990.81	987.51	984.34	980.33	977.27	972.92	968.07	965.91	960.26
$y_{w2}$	24.70	57.74	67.19	78.23	100.78	120.92	137.80	147.07	155.73	166.29	174.60	186.46	199.29	205.46	221.04
$z_{w2}$	37.41	36.58	36.32	36.39	36.20	35.93	35.81	35.91	36.09	35.89	35.94	35.80	36.02	36.05	35.93
$x_{w3}$	1031.10	1019.13	1015.84	1011.80	1003.76	996.31	989.97	986.84	983.85	979.87	976.71	971.97	967.45	965.37	959.34
$y_{w3}$	43.27	76.36	86.24	96.94	120.13	140.46	156.70	166.41	174.89	185.57	194.14	206.13	218.65	225.10	241.18
$z_{w3}$	47.53	46.75	46.71	46.61	46.74	46.62	46.18	46.49	46.54	46.40	46.61	46.60	46.60	46.76	46.98

Table 1. The measurement results of a welding seam of type V

Row 1 was the sequence number of measurement points. Row 2 was one of outside edges of the seam. Row 4 was another. Row 3 was its bottom edge. All data were with unit mm in the world frame. The measurement errors were in the range  $\pm 0.2\text{mm}$ . The measurement results are also shown in the world frame and *XOY* plane in Fig. 4 respectively. Fig. 4 is the data graph shown in 3D space, and Fig. 4 on *XOY* plane in frame *W*. It can be seen that the results were well coincided with the edge lines of the seam (Xu & Tan, 2004).



(a) 3D space



(b) XOY plane

Figure 4. The data graph of vision measurement results of a type V welding seam

## 4. Feature extraction based on second order difference

### 4.1 Image pre-processing

The gray image of laser stripe is captured via a camera with light filter. Generally, its size is large. For example, it could be as large as 576×768 pixels. Therefore, simple and efficient image pre-processing is essential to improve visual control performance in real time. The image pre-processing includes image segmentation, image enhancement and binarization (Xu et al., 2004a; 2004b).

#### 4.1.1 Image segmentation

First, the background gray value of the image is counted. Along its horizontal and perpendicular direction, lines with constant space are drawn. Gray values of all pixels on the lines are added, and its average value is taken as the gray value of background. It is given in (18).

$$\begin{cases} B = \frac{1}{n_w n_1 + n_h n_2} \left( \sum_{i=1}^{n_w} \sum_{j=1}^{n_1} I(i, 10j) + \sum_{i=1}^{n_2} \sum_{j=1}^{n_h} I(10i, j) \right) \\ n_1 = \text{Int}(n_h/10), n_2 = \text{Int}(n_w/10) \end{cases} \quad (18)$$

where  $n_w$  and  $n_h$  are the image width and height respectively,  $n_1$  is the number of horizontal lines,  $n_2$  is the number of vertical lines, and  $I(x, y)$  is the gray value of the pixel in coordinates  $(x, y)$ .

Usually, laser stripe has higher brightness than the background. Along the lines drawn above, all pixels with gray value greater than  $B+T_1$  are recorded. The target area on the image is confirmed according to the maximum and the minimum coordinates of pixels recorded along the horizontal and perpendicular direction respectively.

$$\begin{cases} X_1 = \text{Min}\{i : I(i, 10j_1) - B > T_1 \text{ or } I(10i_1, j) - B > T_1\} \\ X_2 = \text{Max}\{i : I(i, 10j_1) - B > T_1 \text{ or } I(10i_1, j) - B > T_1\} \\ Y_1 = \text{Min}\{j : I(i, 10j_1) - B > T_1 \text{ or } I(10i_1, j) - B > T_1\} \\ Y_2 = \text{Max}\{j : I(i, 10j_1) - B > T_1 \text{ or } I(10i_1, j) - B > T_1\} \\ 1 \leq i \leq n_w, 1 \leq j \leq n_h, i_1 = \text{INT}(i/10), j_1 = \text{INT}(j/10) \end{cases} \quad (19)$$

where  $T_1$  is the gray threshold. The target area consists of  $X_1, X_2, Y_1$  and  $Y_2$ . The structured light image is suffered from arc light, splash, and acutely changed background brightness during welding. As known, the intensity of the arc light and splash changes rapidly, but the laser intensity keeps stable. According to this fact, the effect of arc light and splash can be partly eliminated via taking the least gray value between sequent images as the new gray

value of the image.

$$I(i, j) = \text{Min}\{I_k(i, j), I_{k-1}(i, j)\} \quad (20)$$

where  $I_k$  is the image captured at  $k$ -th times, and  $I_{k-1}$  is  $k-1$ -th.  $X_1 \leq i \leq X_2$ ,  $Y_1 \leq j \leq Y_2$ .

#### 4.1.2 Image enhancement and binarization

The target area is divided into several parts, and its gray values are divided into 25 levels. For every part, the appearance frequency of every gray level is calculated, as given in (21).

$$\begin{cases} F(k, h) = \sum_{i=X_1}^{X_2} \sum_{j=Y_1}^{Y_2} P(k, h) \\ P(k, h) = \begin{cases} 1 & k = \text{Int}(i/5), h = \text{Int}(I(i, j)/10) \\ 0 & \text{others} \end{cases} \end{cases} \quad (21)$$

Taking into account the different contrast between the laser stripe and background, the gray value with higher level, whose appearance reaches specified frequency, is regarded as the image enhancement threshold  $T_2(k)$ .

$$T_2(k) = 10K, \text{ iff } \left( \sum_{h=25}^K F(k, h) > S_1 \right) \vee (F(k, K) > S_2) \quad (22)$$

where  $S_1$  is the specified sum of the frequency with the higher gray level,  $S_2$  is the specified frequency with higher level in one child area, and  $K$  is the gray level,  $1 \leq K \leq 25$ .

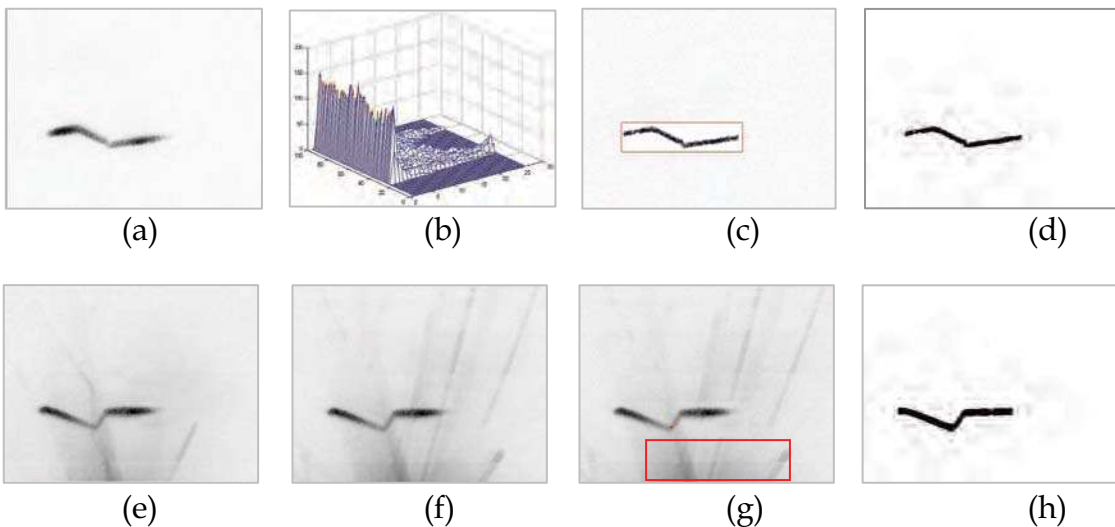


Figure 5. The primary image, frequency distribution map and object segmentation

According to the threshold of every child area, high-pass filter and image enhancement are applied to the target area, followed by Gauss filter and binary thresholding. Fig. 5 is the result of image segmentation of a welding seam. In detail, Fig. 5(a) is the original image with inverse colour, Fig. 5(b) shows its distribution of gray frequency, Fig. 5(c) is the image of the strengthened target area, and Fig. 5(d) is the binary image. Fig. 5(e) and Fig. 5(f) are two frames of original images with inverse colour in sequence during welding, and Fig. 5(g) is the processing result via taking the least gray value in the target area with (20). Fig. 5(h) is its binary image. It can be seen that the binary images of welding seams, obtained after image pre-processing with the proposed method, are satisfactory.

## 4.2 Features extraction

Because the turning points of the laser stripe are the brim points of the welding seam, they are selected as the feature points. To adjust the pose of the weld torch easily, some points on the weld plane are required. Therefore, the goal of features extraction is to search such turning points and weld plane points from the binary image.

To thin the binary image of welding seam, the average location between the upper edge and the lower one, which is detected from the binary image, is regarded as the middle line of laser stripe. Fig. 6(a) shows the upper, lower edge, and middle line of the laser stripe. Because of the roughness of the binary laser stripe, the middle line curve has noise with high frequency, seen in the bottom of Fig. 6(b).

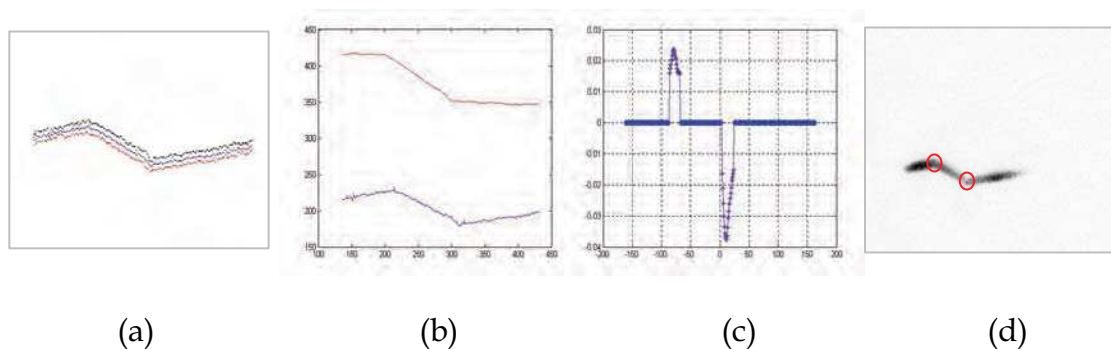


Figure 6. The procedure of features extraction

The middle line stored in an array with two dimensions is transformed via Houghing transformation, to make its feature direction same as the  $x$ -axis. Houghing transformation is shortly described as follows.

First, the position vector of the average of all points on the middle line is computed.

$$\bar{m}_d = \frac{1}{N} \sum_{i=1}^N m_d(i) \quad (23)$$

where  $N$  is the point number on the middle line, and  $\bar{m}_d$  is the position vector of the average,  $\bar{m}_d = [\bar{m}_d(1) \ \bar{m}_d(2)]^T$ .  $m_d(i,1)$  is the coordinate  $x$  of the  $i$ -th point, and  $m_d(i,2)$  is the coordinate  $y$ .

Second, the position vector of each point on the middle line after Hotelling transformation is calculated.

$$C_d = \frac{1}{N} \sum_{i=1}^N m_d(i)m_d(i)^T - \bar{m}_d\bar{m}_d^T \quad (24)$$

$$m_{dh}(i) = V[m_d(i) - \bar{m}_d] \quad (25)$$

where  $m_{dh}(i) = [m_{dh}(i,1) \ m_{dh}(i,2)]^T$  is the position vector of the  $i$ -th point on the middle line after Hotelling transformation.  $V$  is the eigenvector matrix of  $C_d$ , whose first row has large eigenvalue.

To clear up the effect of high frequency noise, the middle line after Hotelling transformation should be filtered. In the condition to keep the  $x$ -coordinate invariable,  $y$ -coordinate is filtered using Takagi-Sugeno fuzzy algorithm, given by equation (26) and (27).

$$\tilde{m}_{dh}(k,2) = \left[ \sum_{h=-5}^5 m_{dh}(k-h,2)\mu(h) \right] / \sum_{h=-5}^5 \mu(h) \quad (26)$$

where  $\tilde{m}_{dh}(k,2)$  is the  $y$ -coordinate of the  $k$ -th point on the filtered middle line.  $\mu(h)$  is the membership function.

$$\mu(h) = \begin{cases} 1 & -3 \leq h \leq 3 \\ 2 - |h|/3 & 3 < |h| \leq 5 \\ 0 & |h| > 5 \end{cases} \quad (27)$$

A line gained by Hough transform, which is the closest to the  $x$ -axis direction converted by Hotelling transformation, is viewed as the main line. Locations of points on the middle line are mapped into the parameter space  $A(p, q)$  of the line function, shown in (28), and the  $(p, q)$  with the maximum value of  $A$  is the

parameter of the main line. All points on the middle line satisfied with the main line function are feature points of the weld plane.

$$\begin{cases} A(p, q) = \sum_{k=1}^M \sum_{p=pMin}^{pMax} B(p, q) \\ B(p, q) = \begin{cases} 1 & q = -p\tilde{m}_{dh}(k,1) + \tilde{m}_{dh}(k,2) \\ 0 & \text{others} \end{cases} \end{cases} \quad (28)$$

The main line is rotated an angle in order to make it parallel to the  $x$ -axis direction.

$$m_{dr}(i) = V_1 \tilde{m}_{dh}(i) = \begin{bmatrix} \cos \theta & -\sin \theta \\ \sin \theta & \cos \theta \end{bmatrix} \tilde{m}_{dh}(i) \quad (29)$$

where  $\theta = \text{atan}(p)$  is the inclination angle between the main line and  $x$ -axis,  $m_{dr}(i)$  is the position vector of the  $i$ -th point on the rotated middle line,  $V_1$  is a rotation matrix formed with  $\cos \theta$  and  $\sin \theta$ .

The point with the maximum of the local second derivative is the turning point of the middle line. After reverse transform as given in (30), the position of the welding seam feature point in the original image is obtained.

$$m_{dm}(i) = V^{-1} V_1^{-1} m_{drm}(i) + \bar{m}_d \quad (30)$$

where  $m_{drm}(i)$  is the position vector of the  $i$ -th turning point on the middle line, and  $m_{dm}(i)$  is the turning point position in the original image.

The curve at the top of Fig. 6(b) shows the middle line after filtered and transformed. The second derivative of the middle line is seen in Fig. 6(c). Two feature points of the welding seam on the original image can be read from Fig. 6(d).

## 5. Feature extraction based on geometric centre

### 5.1 Algorithms for profiles extraction

Fig. 7 shows two frames of laser images of a welding seam of type V groove, in which Fig. 7(a) is an original image before welding, and Fig. 7(b) is an image with reflection of laser on the surface of the welding seam after root pass welding. It can be found that the two images are different in a very large degree. So they should be dealt with different strategies. The method proposed in Section 4 is difficult to deal with the image as given in Fig. 7(b). However, the two im-

ages have a common property, that is, the area of the welding seam is just part of the image. So the welding seam area should be detected to reduce the computation cost (Li et al., 2005).

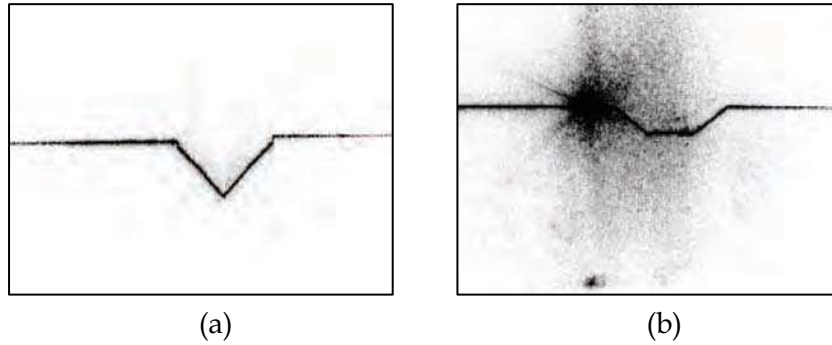


Figure 7. Images of welding seams before and after root pass welding

### 5.1.1 Welding seam area detection

In order to reduce the computational time required in image processing, only the image of welding seam area is processed. However, some disturbances such as reflection shown in Fig. 7(b) will be segmented in the object area with the method in Section 4, which increases the difficulty of features extraction later. Here, an intensity distribution method is presented to detect the object area. The laser stripes shown in Fig. 7, captured by another visual sensor, are horizontal; their range in column is almost from the first to end. So only the range in row needs to be detected. It can be determined by calculating the distribution of intensity of pixels in row. Apparently, the main peak of intensity is nearby to the position of the main vector of laser stripe. So the range of seams in Y-axis direction of the image plane can be detected reliably with (31).

$$\begin{cases} Y_2 = \text{Min}\{Y_p + h_w + m_w, n_h\} \\ Y_1 = \text{Max}\{Y_p - m_w, 0\} \end{cases} \quad (31)$$

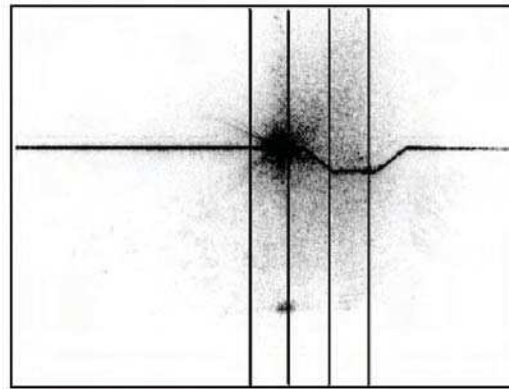
where  $Y_p$  is the Y-coordinate of main vector;  $h_w$  is the height of welding groove; and  $m_w$  is the margin remained. The target area consists of 0,  $n_w$ ,  $Y_1$  and  $Y_2$ .

### 5.1.2 Column based processing

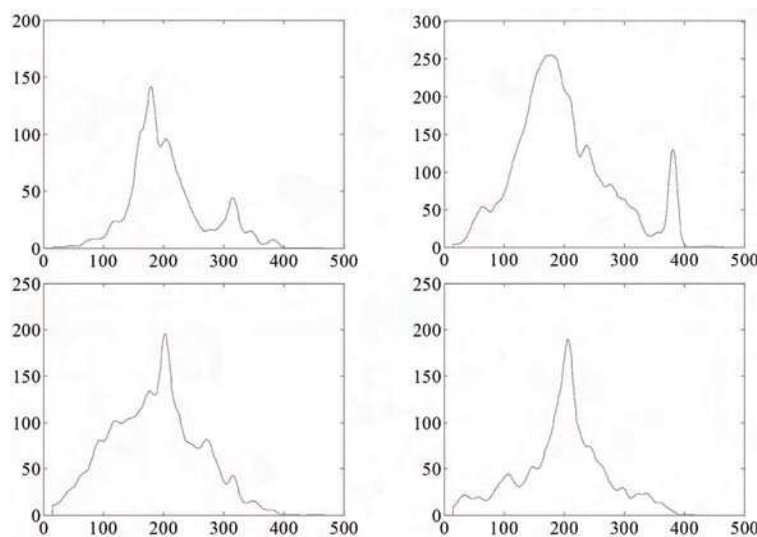
Column based profiles extraction calculates the distribution of pixels' intensity with columns to get the points of profile. Some algorithms such as multi-peak method and centre of gravity (Haug & Pristrchow, 1998), gradient detection and average of upper edges and the lower edges in Section 4 are all effective



for the task. In order to get high quality profiles of seams, a method that combines smoothing filter, maximum detection and neighbourhood criteria is proposed.



(a)



(b)

Figure 8. Intensity extraction of four columns

Firstly, a low pass filter is designed to smooth the intensity curve of column  $i$ . Usually, the pixels of profiles are in the area of main peak, and the peaks caused by disturbances are lower or thinner. After smoothing the intensity curve, the plateau is smoothed with one maximum in main peak, and the lower or thinner peaks are smoothed into hypo-peaks. Fig. 8 gives an example of intensity distribution of column 300, 350, 400, 450 of a welding seam image. Fig. 8(a) shows the original image and the positions of four example columns. Fig. 8(b) shows their intensity distribution.

## Thank You for previewing this eBook

You can read the full version of this eBook in different formats:

- HTML (Free /Available to everyone)
- PDF / TXT (Available to V.I.P. members. Free Standard members can access up to 5 PDF/TXT eBooks per month each month)
- Epub & Mobipocket (Exclusive to V.I.P. members)

To download this full book, simply select the format you desire below

